Efficient Visualization Method of Buckling Region in Dynamic Transient Analysis of Cable Network Structures

By Shoko Arita & Yasuyuki Miyazaki

Shizuoka University

Abstract- Deployable structure system using flexible members is necessary to construct a large structure in the space. The flexible members easily buckle as seen in wrinkles and slack. Therefore, it is available at designing of spacecraft to grasp when, where and how large the buckling occurs in the entire structure during the deployment. When dynamic analysis of large flexible structures which can ignore bending is conducted, the truss element and the membrane element, which do not consider the bending of an element, are often used from the viewpoint of calculation cost. Therefore, this paper proposes a comprehensive and efficient visualization method of buckling occurrence region and buckling magnitude during dynamic response analysis using the truss element to progress convenience in design. The method proposed in this paper is based on two previous studies. The proposed method is verified by a simple truss model, and an application example is shown.

Keywords: deployable structures, buckling, visualization, fem, truss element, dynamic structural analysis, transient response.

GJRE-J Classification: FOR Code: 090199

Strictly as per the compliance and regulations of:

Efficient Visualization Method of Buckling Region in Dynamic Transient Analysis of Cable Network Structures

Shoko Arita [α] & Yasuyuki Miyazaki [σ]

Abstract- Deployable structure system using flexible members is necessary to construct a large structure in the space. The flexible members easily buckle as seen in wrinkles and slack. Therefore, it is available at designing of spacecraft to grasp when, where and how large the buckling occurs in the entire structure during the deployment. When dynamic analysis of large flexible structures which can ignore bending is conducted, the truss element and the membrane element, which do not consider the bending of an element, are often used from the viewpoint of calculation cost. Therefore, this paper proposes a comprehensive and efficient visualization method of buckling occurrence region and buckling magnitude during dynamic response analysis using the truss element to progress convenience in design. The method proposed in this paper is based on two previous studies. The proposed method is verified by a simple truss model, and an application example is shown.

Keywords: deployable structures, buckling, visualization, fem, truss element, dynamic structural analysis, transient response.

I. Background

A deployable structure largely deforms from moment to moment in the deployment process, and the flexible member easily buckles as seen in wrinkles and slack of the membrane surface, for instance. Buckling such as unexpected wrinkle or slack has a problem of deteriorating the surface accuracy of the deployed film surface. On the other hand, a folded structure made of flexible member is usually easier to deploy than rigid member because stress concentration occurring at a corner of fold is mitigated by out-of-plane deformation, which is easier to occur in a flexible member such as slack on a membrane. That is a major reason to use flexible members as deployable space structures.

Analysis of the dynamic behavior of flexible structures is necessary for the design and development of such deployable structures. Flexible members such as membranes and tethers often can be applied an approximation that ignores bending in the modeling.

From the viewpoint of calculation cost, truss element and membrane element, which do not consider the bending of an element, are often used for analyses of large-scale dynamic FEM (Shirasawa et al., 2011; Ono et al., 2014).However, there are few studies that efficiently detect buckling from the entire structure during response analysis using the element model which does not consider bending. Because solution of buckling analysis is generally acquired from equation of bending moment. Therefore, the authors have proposed and developed a method to detect wrinkle and slack using the membrane elements (Arita et al., 2014) and a method to detect snap through buckling during the dynamic analysis using the truss element (Arita and Miyazaki, 2018). This paper proposes a comprehensive and efficient visualization method of buckling occurrence region and buckling magnitude during dynamic response analysis by using these two theories to progress convenience in actual design of gossamer spacecraft. By visualizing the buckling region, it is expected at actual designing that it will be easier to specify the part where buckling easily occurs, and to control or deal with the buckling part. A general method of visualization of buckling is to display the buckling mode shape in order to examining the buckling load and the shape after buckling (Noguchi and Fujii, 2000; Ikeda dt al., 2003). On the other hand, the purpose of the method proposed in this paper is not to obtain the mode shape but to grasp comprehensively when and what area the buckling displacement occurs during transient response of the deployment. Visualization based on such a concept is a unique point of this research. In a previous study, a method using tension field theory has been proposed as a method of calculating the amount of deformation after buckling (Conci, 2007).However, it is pointed that the assumption of tension field theory does not establish for the buckling of flexible structures (Iwasa et al., 2004).Therefore, the method proposed in this paper is to calculate the buckling displacement amount without using the tension field theory.

The theory of the visualization method is shown in Section 2. Section 3 shows the results of verification of the proposed method by a simple truss model, and Section 4 shows an analysis example assuming development of flexible membrane.

Author α: Department of Mechanical Engineering, Faculty of Engineering, Shizuoka University 3-5-1 Johoku, Naka-ku, Hamamatsu, Shizuoka, 432-8011, Japan. e-mail: arita.shoko@shizuoka.ac.jp
Author σ: Department of Aerospace Engineering, College of Science and Technology, Nihon University 7-24-1 Narashinodai, Funabashi, Chiba, 274-8501, Japan.

II. Theories of Buckling Analysis and Visualization

In the proposed method, the dynamic response of the entire structure is analyzed by the truss element, and the amount of the snap through buckling displacement of the node is visualized by color contour. However, since the truss element cannot express the deformation other than in the axial direction, it is necessary to calculate the long column buckling of the element itself in order to grasp the comprehensive buckling of the entire structure. Since a flexible member such as a membrane has a characteristic that compression rigidity is very small compared with tension and it is easy to buckle, it is necessary to devise modeling of the compressive stiffness in post buckling analysis. Hence, we adopt the theory called Mod-SRM, which models appropriately such features, to detect and visualize the buckling of each truss element. In other words, this paper proposes the method to visualize the comprehensive buckling of the entire structure by displaying the color contour of the snap through buckling of nodes and the long column buckling of elements with respect to the dynamic transient response diagram of the truss element. In this chapter, the detection and visualization method of the snap through buckling of nodes is explained in Section 2.1, and the detection and visualization method of the long column buckling of elements by Mod-SRM is explained in Section 2.2.

a) Snap through Buckling of Nodes in Truss Elements

  i. *Introduction of Buckling Detection and Quantification Method*

Only the snap through buckling of the node is detectable in the truss element. Since detection and quantification of the snap through buckling are described in detail in the previous work (Arita and Miyazaki, 2018) by the authors, in this section, a schematic view of the method is shown in Fig.1 and the outline is explained below.
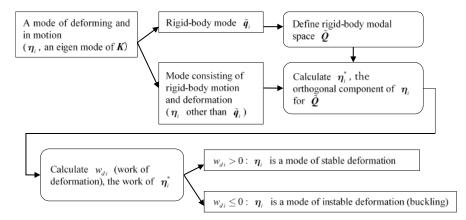

Fig.1: Buckling detection method. After extracting the orthogonal component to the rigid-body modal space $\tilde{Q}$ from each eigen mode of the stiffness matrix K, the eigen mode is judged if buckling or not according to the work of deformation.

Multiple buckling modes often appears at the same time. In such a case, quantification is carried out in order to determine the most likely buckling mode considering the motion state of the structure. Assuming that buckling displacement Δx is caused by external disturbance force ΔF, ΔF is obtained by solving the equation of motion. Then, the norm of the obtained ΔF is defined as a validation parameter "DF value". It is determined that the mode with the smallest DF value is the most likely buckling mode. Moreover, the norm of the buckling displacement Δx is also defined as another validation parameter "BD value".

  ii. *Visualization of Buckling of Nodes Based on Buckling Displacement*

In this section, the authors propose a method of visualization using the detected buckling mode and the BD value explained above. The visualization method is to display the amount of the snap through buckling displacement of each node is visualized by color contour for the most likely buckling mode.

The element used in this theory is a two-node truss element having three degrees of freedom of x, y, z per node. We define n as the number of nodes of the entire structure, and define h as the most likely buckling mode. h is a normalized vector, in which the proportion of x, y and z displacements of each node is arranged. Then, the component corresponding to (x, y, z) of the j th node in h is defined as (x_j, y_j, z_j), and h_j is defined as follows.

$$h_j \ ^{\circ} \ [x_j, y_j, z_j]^T \tag{1}$$

Likewise, a subscript j is written with respect to values of j th node. Here, we extract only buckling nodes from the buckling mode in order to extract local

buckling by calculating the work for each node. Nodes of which deformation work becomes 0 or less are considered as buckling nodes because the displacement proceed by negative deformation work. To calculate the deformation work, it is necessary to extract only the deformation component from the mode that includes rigid-body motion. The orthogonal component $\boldsymbol{h}^*$ to the rigid-body modal space $\tilde{\boldsymbol{Q}}$, which means the deformation component, is extracted by Eq. (2). The deformation work of each node w_j^* in the buckling mode $\boldsymbol{h}_j$ is calculated by using the stiffness matrix $\boldsymbol{K}$ as Eq. (3).

$$\boldsymbol{h}^* = \boldsymbol{h} - \sum_{k=1}^{n} \frac{(\boldsymbol{h} \cdot \tilde{\boldsymbol{q}}_k)}{(\tilde{\boldsymbol{q}}_k \cdot \tilde{\boldsymbol{q}}_k)} \boldsymbol{q}_k \qquad (2)$$

$$w_j^* = \boldsymbol{h}_j^* \cdot \left(\boldsymbol{K} \boldsymbol{h}^* \right)_j \qquad (3)$$

Buckling displacement amount (BD value) is calculated for the node of which w_j^* is 0 or less by Eq. (4). α is a scalar giving the magnitude of the displacement in the buckling mode direction, and the details are explained in the previous study (Arita and Miyazaki, 2016). Therefore, only the results are shown here.

$$BD = \alpha |\boldsymbol{h}_j| \qquad (4)$$

$$\alpha = \frac{\boldsymbol{a} \cdot \boldsymbol{b} + \boldsymbol{a} \cdot \boldsymbol{c}}{|\boldsymbol{a}|^2} \qquad (5)$$

where

$$\boldsymbol{a} = \frac{1}{\beta \Delta t^2}(\boldsymbol{I} - \tilde{\boldsymbol{Q}}[\tilde{\boldsymbol{Q}}^T \tilde{\boldsymbol{Q}}]^{-1} \tilde{\boldsymbol{Q}}^T)\boldsymbol{M}\boldsymbol{h}$$

$$\boldsymbol{b} = \frac{1}{\beta \Delta t}(\boldsymbol{I} - \tilde{\boldsymbol{Q}}[\tilde{\boldsymbol{Q}}^T \tilde{\boldsymbol{Q}}]^{-1} \tilde{\boldsymbol{Q}}^T)\boldsymbol{M}\dot{\boldsymbol{x}}_0 \qquad (6)$$

$$\boldsymbol{c} = \frac{1}{2}(\boldsymbol{I} - \tilde{\boldsymbol{Q}}[\tilde{\boldsymbol{Q}}^T \tilde{\boldsymbol{Q}}]^{-1} \tilde{\boldsymbol{Q}}^T)\boldsymbol{M}\ddot{\boldsymbol{x}}_0$$

b is the coefficient of the Newmark-β method, Dt is the time step width in the time integration of the

Newmark-β method, $\boldsymbol{M}$ is the mass matrix, $\dot{\boldsymbol{x}}_0$ and $\ddot{\boldsymbol{x}}_0$ are the velocity and acceleration of the previous time step respectively. Note that although Newmark-β method was used in the previous paper (Arita and Miyazaki, 2016), the concept of this method is also effective for other numerical integration methods, and similar equations can be derived by other methods. The magnitude of the displacement by the buckling is visualized by color contour display of nodes according to the BD value.

b) *Long Column Buckling of Elements in Truss Elements*

i. *Introduction of Mod-SRM*

A flexible member is easy to buckle because the compressive stiffness of the flexible member is very small compared to tensile stiffness. Therefore, methods that determine the compressive stiffness by multiplying the tensile stiffness by a coefficient smaller than 1 has been proposed for the element model that does not consider bending (e.g. Miyazaki, 2006). Mod-SRM, which is one of them, proposed to be able to determine the compressive stiffness ratio uniquely according to the amount of the out-of-plane buckling by introducing the stretchable elastic theory into the element model (Arita et al., 2014). Because Mod-SRM is based on the bending deformation of a beam, the visualization method proposed this paper is to apply Mod-SRM to the truss element. The outline of Mod-SRM and the derivation of physical quantities for the visualization are introduced in this section.

First of all, supposing one truss element of which total length is defined $l/2$ deforms like a slack of a cable, the equilibrium equation is expressed as Eq.(7) in an infinitesimal line element $d\boldsymbol{x}$ subjected to the load $\boldsymbol{P}$ as shown in Fig. 2. Eventually, Eq.(8) and (9)are obtained from the equilibrium equation. Details of this derivation are written in the previous work (Arita et al., 2014).
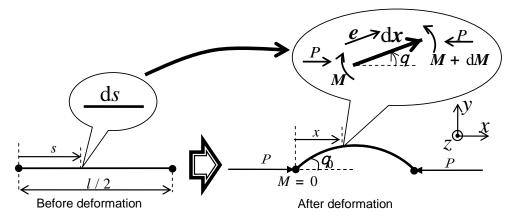

Fig. 2: Mathematical modeling of Mod-SRM. Supposing one truss element deforms like a slack of a cable, the equilibrium of forces and moments are obtained in an infinitesimal line element $d\boldsymbol{x}$ subjected to the load $\boldsymbol{P}$.

$$EI\frac{\mathrm{d}^2\theta}{\mathrm{d}s^2}+\left(1-\frac{P\cos\theta}{EA}\right)P\sin\theta=0 \tag{7}$$

$$\int_0^\pi f(t)\,\mathrm{d}t=\pi\sqrt{\frac{\eta}{2}} \tag{8}$$

$$\int_0^\pi (1-\eta\lambda C_\theta)C_\theta f(t)\,\mathrm{d}t=(1-\varepsilon)\pi\sqrt{\frac{\eta}{2}} \tag{9}$$

ε is the equivalent in-plane compressive strain, defined as shown in Fig.3. E^* means Young's modulus after buckling, and α denotes the ratio of stiffness in the compressive direction to the tensile direction. l is a material constant and is defined by Eq. (10). η is a non dimensional compressive load and is defined by Eq. (11). E means Young's modulus, A means cross-sectional area and I means moment of inertia of area. C_q and $f(t)$ are functions defined by Eq. (12) and (13) respectively. The compressive stiffness ratio α is obtained by Eq. (14):

$$\lambda\equiv\frac{EI\pi^2}{EAl^2} \tag{10}$$

$$\eta\equiv\frac{P}{\left(\dfrac{EI\pi^2}{l^2}\right)} \tag{11}$$

$$\cos\theta=\frac{1+\cos\theta_0}{2}-\frac{1-\cos\theta_0}{2}\cos t\equiv C_\theta(t)$$
$$\begin{cases}\theta:\theta_0\to 0\\ t:0\to\pi\end{cases} \tag{12}$$

$$f(t)\equiv\frac{1}{\sqrt{(1+C_\theta)\left[1-\dfrac{\eta\lambda}{2}(C_\theta+\cos\theta_0)\right]}} \tag{13}$$

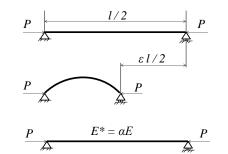$$\alpha=\frac{P}{EA\varepsilon}=\frac{\eta\lambda}{\varepsilon} \tag{14}$$

Fig. 3: Definition of symbols. ε is the equivalent in-plane compressive strain, E^* is Young's modulus after buckling, and α is the compressive stiffness ratio.

That is to say, given the equivalent plane compressive strain ε and the material constant l, the relation between the non-dimensional compressive load η and strain ε can be obtained when the load η and

angle θ_0 are determined under Eq.(8) and (9).In the actual calculation, θ_0 is given and h is obtained by Newton's method so as to satisfy Eq. (8), and ε is obtained by Eq. (15):

$$\varepsilon=1-\frac{\displaystyle\int_0^\pi(1-\eta\lambda C_\theta)C_\theta f(t)\,\mathrm{d}t}{\displaystyle\int_0^\pi f(t)\,\mathrm{d}t} \tag{15}$$

It is convenient to calculate the approximation of η as the polynomial of ε by using the relation obtained by Eq. (15) in advance, and in the transient response analysis, η is calculated from the polynomial according to the value of ε at the time step. Hence, the compressive stiffness ratio α is decided every time step by Eq. (14).

ii. *Visualization of Buckling of Elements Based on Buckling Displacement*

In visualization, the buckling of each element is judged and the buckling elements are displayed in color contour according to the magnitude of ε.

The calculated value of compressive buckling load is used for the judgement of the buckling. In general, when an axial compressive load P is applied to a simply supported beam at both ends of bending stiffness EI and length l shown in Fig. 4, the Euler buckling load P_{0cr} is obtained as Eq. (17) from Eq. (16), which is the equilibrium equation assuming no expansion, contraction and shear deformation.
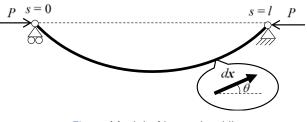

Fig. 4: Model of beam buckling

$$EI\frac{\mathrm{d}^2\theta}{\mathrm{d}s^2}+P\sin\theta=0 \tag{16}$$

$$P_{0cr}=\frac{EI\pi^2}{l^2} \tag{17}$$

On the other hand, considering expansion and contraction and shear deformation, if the equilibrium equation can be written as Eq. (18), the buckling load P_{cr} is written as Eq.(19).

$$EI\frac{\mathrm{d}^2\theta}{\mathrm{d}s^2}+Pf(\theta)\sin\theta=0 \tag{18}$$

$$P_{cr}=\frac{P_{0cr}}{f(0)} \tag{19}$$

This is proved as follows;

Multiplying both sides of Eq. (18) by $\dfrac{d\theta}{ds}$ gives the following equation;

$$EI\frac{d^2\theta}{ds^2}\frac{d\theta}{ds} + Pf(\theta)\sin\theta\frac{d\theta}{ds} = 0 \tag{20}$$

Determining θ_0 as the θ at the point where the bending moment becomes 0, the following is obtained by integration by θ of Eq. (20);

$$\frac{1}{2}EI\left(\frac{d\theta}{ds}\right)^2 + P\int_{-\theta_0}^{\theta} f(\theta)\sin\theta d\theta = 0$$

$$\Rightarrow \frac{d\theta}{ds} = \sqrt{\frac{2P}{EI}\int_{-\theta_0}^{\theta} -f(\theta)\sin\theta d\theta} \tag{21}$$

The integral term in the Eq. (21) can be written as below;

$$\int_{-\theta_0}^{\theta} -f(\theta)\sin\theta d\theta = \cos\theta f(\theta) - \cos(-\theta_0)f(-\theta_0) - \int_{-\theta_0}^{\theta} f'(\theta)\cos\theta d\theta$$

$$= \cos\theta f(\theta) - \cos\theta_0 f(-\theta_0) - \int_{-\theta_0}^{\theta} f'(\theta)\cos\theta d\theta$$

$$+ \cos\theta_0 f(-\theta_0) - \cos\theta_0 f(\theta) + \int_{-\theta_0}^{\theta} \cos\theta_0 f'(\theta)d\theta \tag{22}$$

$$= (\cos\theta - \cos\theta_0)f(\theta) - \int_{-\theta_0}^{\theta} (\cos\theta - \cos\theta_0)f'(\theta)\cos\theta d\theta$$

Here, the following variable transformation is defined;

$$\cos\theta = C(u) = \frac{1+\cos\theta_0}{2} + \frac{1-\cos\theta_0}{2}\cos u$$

$$\begin{cases} \theta : -\theta_0 \to \theta_0 \\ u : -\pi \to \pi \end{cases} \tag{23}$$

The following equation is obtained from Eq. (23);

$$\frac{du}{d\theta} = \frac{\sqrt{1+C(u)}}{\sqrt{C(u)-\cos\theta_0}} \tag{24}$$

Using Eq. (21), (22) and (23), the following relation is obtained:

$$\frac{du}{ds} = \frac{du}{d\theta}\frac{d\theta}{ds}$$

$$= \sqrt{\frac{2P}{EI}(1+C(u))\left\{ f(\theta) - \frac{1}{C(u)-\cos\theta_0}\int_{-\theta_0}^{\theta} (C(u)-\cos\theta_0)f'(\theta)d\theta \right\}} \tag{25}$$

$$\equiv \sqrt{\frac{2P}{EI}(1+C(u))\{f(\theta)-h(u)\}}$$

Furthermore, using Eq. (23) and (24), the $h(u)$ is written as below;

$$h(u) = \frac{1}{C(u)-\cos\theta_0}\int_{-\theta_0}^{\theta} (C(u)-\cos\theta_0)f'(\theta)d\theta$$

$$= \frac{2}{(1-\cos\theta_0)(1+\cos u)}\int_{-\theta_0}^{\theta} \frac{(1-\cos\theta_0)(1+\cos u)}{2} f'(\theta)d\theta$$

$$= \frac{1}{1+\cos u}\int_{-\pi}^{u} (1+\cos v)f'(\theta(v))\frac{\sqrt{C(v)-\cos\theta_0}}{\sqrt{1+C(v)}} dv \tag{26}$$

$$= \sqrt{\frac{1-\cos\theta_0}{2}}\int_{-\pi}^{u} \frac{(1+\cos v)^{\frac{3}{2}}}{1+\cos u}\frac{f'(\theta(v))}{\sqrt{1+C(v)}} dv$$

Because $\theta_0 \to 0$ in the case of buckling, the values of $C(u)$, θ and $h(u)$ are as follows;

$$C(u) \to 1 , \quad \theta \to 0 , \quad h(u) \to 0 \tag{27}$$

Thus, Eq. (19) is derived by Eq. (25) as follows;

$$\frac{2\pi}{l} = \sqrt{\frac{2P^{cr}}{EI} 2f(0)}$$
$$\Rightarrow P^{cr} = \frac{EI\pi^2}{l^2 f(0)} \tag{28}$$

Q.E.D.

In the case of Mod-SRM, the equilibrium equation is Eq. (7). Therefore, P_{cr} is below;

$$f(0) = 1 - \frac{P\cos\theta}{EA} = 1 - \frac{P_{cr}}{EA} \quad (\because \theta = 0 \text{ at the buckling})$$
$$\Rightarrow P_{cr} = \frac{EA(1-\sqrt{1-4\lambda})}{2} \tag{29}$$

where P_{cr} is smaller of the two solutions. From Eq. (11), η_{cr} is below;

$$\eta_{cr} = \frac{2}{1+\sqrt{1-4\lambda}} \tag{30}$$

The same solution is obtained by setting $\theta_0 = 0$ in Eq.(8) and (13). When $\theta_0 = 0$,

$$C_\theta = \cos\theta_0 = 1 \tag{31}$$

Therefore,

$$f(t) = \frac{1}{\sqrt{2(1-\eta\lambda)}} \tag{32}$$

Thus, applying it to Eq.(8),

$$\frac{\pi}{\sqrt{2(1-\eta\lambda)}} = \pi\sqrt{\frac{\eta}{2}} \tag{33}$$

Solving this for η,

$$\eta = \frac{2}{1\pm\sqrt{1-4\lambda}} \tag{34}$$

Two solutions are obtained. Since the buckling load is the one with a smaller value, η_{cr} is obtained as Eq. (30).

Incidentally, the buckling strain ε_{cr} is obtained from Eq. (15) as follows.

$$\varepsilon_{cr} = \eta_{cr}\lambda = \frac{2\lambda}{1+\sqrt{1-4\lambda}} \tag{35}$$

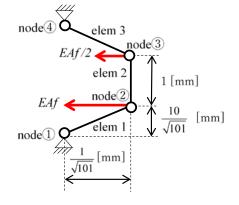## III. VERIFICATION OF VISUALIZATION OF BUCKLING BY NUMERICAL EXPERIMENT

The authors verified the visualization method with a simple truss model consisting of 3 elements and 4 nodes. The truss model is shown in Fig.5, and its specifications are shown in Table 1. Before transient response and visualization, the relationship and polynomial approximation between η and ε were obtained in advance by Mod-SRM as shown in Fig. 6.The tensile strain is the positive value, and the compressive strain is the negative value. The buckling load of an element was obtained as $\eta_{cr} = 1.000129$ that

is, $P_{cr} = 0.005623[N]$ and $\varepsilon_{cr} = 0.0001285$. Note that the compressive stiffness ratio a is calculated in each time step of the transient response analysis based on the polynomial approximation and Eq. (14). The relationship between α and ε, incidentally, is shown in Fig. 7.

The result of the buckling analysis is shown in Fig. 8. The horizontal axis is the time step. The first vertical axis at the left side is the strain of the element. The second vertical axis at the right side represents the detection result of the snap through buckling of the nodes. Since the nodes ① and ④ are fixed, they are excluded. Figure 8 shows the sharp fluctuation of the

strain after Step 750. It can be considered that the drastic decrease of element stiffness due to compressive buckling causes the sharp fluctuation of the strain. Figure 8 also shows that snap through buckling of the nodes occur from Step 794 onwards. Figure 9 is the enlarged figure of Fig. 8 from Step 794 to Step 805 regarding the strain of the elements. Figure 10 is also the enlarged figure of Fig. 8 regarding the nodes, however, the vertical axis shows not the detection result but the BD value of the buckling nodes. Transient response is shown in Fig.11 as a result of visualization of the buckling. Comparing Fig. 9, 10 and 11, it can be confirmed that the color contour is properly visualized in the response diagram corresponding to the strain of the

elements and the BD value of the nodes where the buckling occurred.

In the previous study, Mod-SRM only defined the compressive stiffness ratio for the post buckling analysis of a membrane. The study of the dynamic buckling of a truss element only quantified the ease of buckling and degree of buckling deformation as representative values for the entire structure. On the other hand, the method proposed in this paper enables visually recognizing where and how large the buckling occurs in a transient analysis by calculating the magnitude of buckling displacement for each node and element.
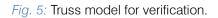

Fig. 5: Truss model for verification.

Table 1: Specifications of the analysis for the truss model.

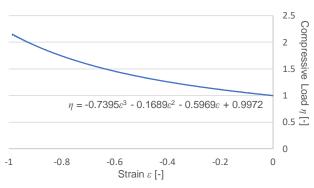| Parameter	Symbol	Value	Unit
time step size	dt	5×10^{-6}	[s]
stiffness of an element	EA	0.55	[N]
density of an element	ρ	1.42	[g/cm³]
increment of external force parameter	$\varDelta f$	2.5×10^{-9}	[-]
condition of constraint:	x,y,z of node①, x,y,z of node④		
condition of loading:	Incresing f step-by-step by $\varDelta f$, node② is subjected to $-EAf$ in the direction of x axis, and node④ is subjected to $-EAf/2$ in the direction of x axis.		

$\eta = -0.7395\varepsilon^3 - 0.1689\varepsilon^2 - 0.5969\varepsilon + 0.9972$

Fig. 6: Relation and polynomial approximation between η and ε. η at each time step in transient response is determined by the polynomial according to ε.
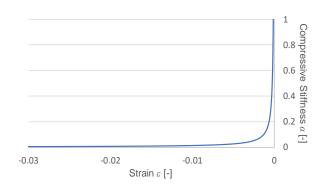
Fig. 7: Relation between α and ε. The compressive stiffness decreases according to the compressive strain.
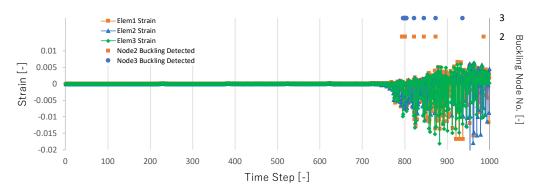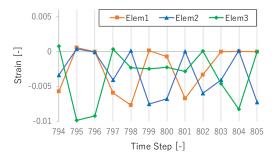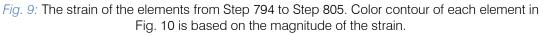

Fig. 8: Result of the buckling analysis. The first vertical axis at the left side is the strain of the element. The second vertical axis at the right side represents the detection result of the snap through buckling of the nodes. The drastic decrease of elements tiff ness due to compressive buckling causes the sharp fluctuation of the strain after Step 750. The snap through buckling of the nodes occur from Step 794 onwards.
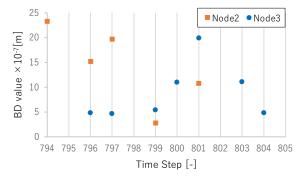

Fig. 9: The strain of the elements from Step 794 to Step 805. Color contour of each element in Fig. 10 is based on the magnitude of the strain.

Fig. 10: BD value of the buckling nodes from Step 794 to Step 805.Color contour of each node in Fig. 10 is based on the magnitude of the BD value.
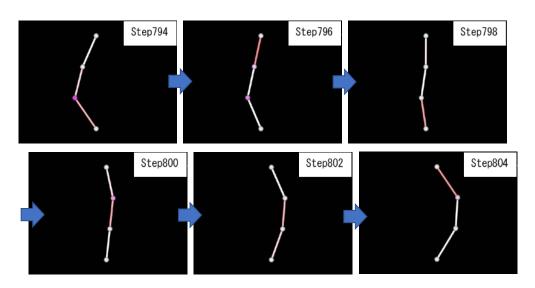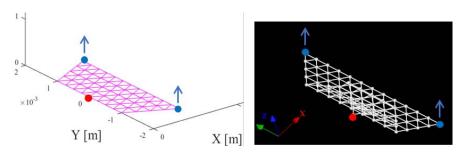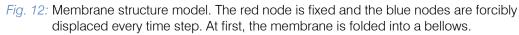
Fig. 11: Transient response and the result of the visualization. Comparing with Fig. 8 and 9, it can be confirmed that the color contour is properly visualized corresponding to the strain of the elements and the BD value of the nodes where the buckling occurred.

IV. Application Example of Membrane Structure

The authors conducted a calculation as an application example with a model assuming that the triangular membrane deploys with booms. The triangular membrane folded into a bellows deploys as shown in Fig. 12 and Table 2. The transient response is shown in Fig. 13. Buckling occurring at the nodes and the elements are visualized, indicating that we can confirm when, where and how large the buckling occurs in the structure.

Fig. 12: Membrane structure model. The red node is fixed and the blue nodes are forcibly displaced every time step. At first, the membrane is folded into a bellows.

Table 2: Specifications of the analysis

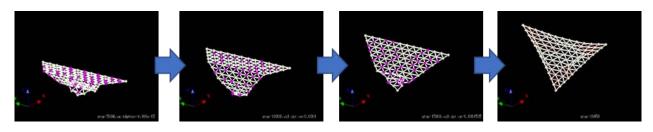| Parameter	Symbol	Value	Unit
time step size	dt	5×10^{-6}	[s]
Young's ratio	E	3.5×10^{9}	[Pa]
Length of an element	l	1×10^{-3}	[m]
Thickness of an element	h	12.5×10^{-6}	[m]
Density of an element	ρ	1.42	[g/cm^3]
Boundary Cindition		Fix the red node and forcibly displace the two blue nodes by 0.75×10^{-7} per time step in the +z direction.	

Fig. 13: Transient response and the result of the visualization. Snap through buckling occurs everywhere on the membrane, and the buckling of the element occurs intensively at the corners at the end of the deployment.

V. Conclusions

The authors proposed a comprehensive and efficient visualization method of buckling region during dynamic response analysis based on two previous studies to progress convenience in actual design of gossamer spacecraft. The proposed method is verified by a simple truss model, and the calculation of an application example is conducted. The result indicates that using this method, we can confirm when, where and how large the buckling occurs in the structure.

References Références Referencias

1. Arita S. and Miyazaki Y., A study of dynamic evaluation of structural buckling, Mechanical Engineering Letters, Vol 2, No.15-00677 (2016), pp.1-8.
2. Arita S. and Miyazaki Y., Modified method of detecting dynamic buckling, Mechanical Engineering Letters, Vol 4, No.17-00441 (2018), pp.1-8.
3. Arita S., Okumiya T. and Miyazaki Y., Numerical model for prediction of wrinkling behavior on a thin-membrane structure, Mechanical Engineering Journal, Vol.1, No.4, SE0041 (2014), pp.1-16.
4. Conci A., after buckling behavior of thin membranes and textiles based on tension field theory and experiments, Proceedings of Mechanics of Solids in Brazil 2007 (2007), pp.147-159.
5. Ikeda K., Yamakawa Y. and Tsutsumi S., Simulation and interpretation of diffuse mode bifurcation of elastoplastic solids, Journal of the Mechanics and Physics of Solids, Vol. 51, Issue 9 (2003), pp.1649-1673.
6. Iwasa, T., Natori, M.C. and Higuchi, K., Evaluation of Tension Field Theory for Wrinkling Analysis With Respect to the Post-Buckling Study, Journal of Applied Mechanics, Vol.71 (2004), pp.532-540.
7. Miyazaki, Y., Wrinkle/slack model and finite element dynamics of membrane, International Journal for Numerical Methods in Engineering, Vol.66, No.7 (2006), pp.1179-1209.
8. Noguchi H. and Fujii F., Extracting the buckling mode from LDL^T-decomposed stiffness matrix, Advances in Computational Engineering and Sciences, Satya N. Atluri and Frederick W. Brust Eds., Vol. 1 (2000), pp.750-755,Tech Science Press.
9. Ono G., Shintaku K., Shirasawa Y., Mori O., Miyazaki Y. and Matsunaga S., Study of Asynchronous Solar Sail Deployment Using Finite Element Method, Transaction of the Japan Society for Aeronautical and Space Sciences, Aerospace Technology Japan, Vol. 12,Issue ists29 (2014), pp.63-67.
10. Shirasawa Y., Mori O., Miyazaki Y., Sakamoto H., Hasome M., Okuizumi N., Sawada H., Furuya H., Matunaga S. and Natori M., Analysis of Membrane Dynamics using Multi-Particle Method for Solar Sail Demonstrator "IKAROS", Proceedings of 52nd AIAA/ASME/ASCE/AHS/ASC Structures, Structural Dynamics, and Materials Conference, AIAA-2011-1890 (2011), pp.1-14.